Tailored Resonance Dependence on Input Optical Power in Silicon Microring Resonators

Lian-Wee Luo[1,*], Gustavo S. Wiederhecker[1,3], Kyle Preston[1], and Michal Lipson[1,2]
[1]Department of Electrical and Computer Engineering, Cornell University, Ithaca, NY 14853, USA
[2]Kavli Institute at Cornell for Nanoscale Science, Cornell University, Ithaca, NY 14853, USA
[3]Current address: Instituto de Fisica Gleb Wataghin, Universidade Estadual de Campinas,CEP 13083-970, Campinas, Sao Paulo, Brazil
*Email: ll399@cornell.edu

***Abstract* – We demonstrate the ability to tailor the resonance dependence on input power in silicon microring resonators using a passive technique by utilizing two counteracting processes, free carrier dispersion blueshift and thermo-optic redshift. In our fabricated silicon microring resonators, we achieve an effective blueshift, as well as effective redshift. We also design and fabricate a power insenstive silicon microring that has a five-fold improvement in cavity energy handling capability compared to a regular microring.**

I. INTRODUCTION

Silicon microring resonators have revolutionized the field of silicon photonics for on-chip optical interconnects over the past decade as they offer a larger bandwidth, lower power consumption and smaller device footprint in microelectronic chips [1-3]. However, silicon microring resonators have one main drawback, that is, the resonant wavelength shifts with input optical power. At high powers, the stored light in a silicon microring is absorbed via two photon absorption (TPA) and as a result free carriers are generated. This in turn leads to a blueshift of the resonance due to free carrier dispersion (FCD). On the other hand, the generated carriers also lead to free carrier absorption (FCA). The TPA and FCA nonlinear processes, together with the linear surface absorption at the Si/SiO_2 interface, result in the heating of the resonator and cause a redshift in the resonance.

The resonance shift is undesirable most of the times but can be beneficial at times. Therefore, the ability to tailor the microresonator spectral dependence on input power is critical. Here we demonstrate tailored resonance dependence on input power in silicon microring resonators using a passive technique by utilizing two counteracting processes, FCD blueshift and TO redshift.

II. THEORETICAL STUDIES OF RESONANCE DEPENDENCE

In order to control the degree of spectral shift with optical power, we analyze the effective resonance shift $\Delta\lambda$ due to the counteracting effects of FCD and TO processes in the silicon microring resonator (neglecting the minor contribution of TO in the cladding SiO_2) [4, 5]:

$$\Delta\lambda \approx \frac{\lambda_0}{n_g}(\Delta n_{FC} + \Delta n_T), \quad (1)$$

where λ_0 is the resonant wavelength, n_g is the group refractive index of the silicon micoring resonator, and Δn_{FC} and Δn_T are the refractive index changes of Si owing to the FCD and TO effects respectively. In particularly, Δn_{FC} can be enhanced by increasing the density of the generated electrons and holes in the silicon. One of the ways to achieve higher density of electrons and holes is to increase the free carrier lifetime (τ_{FC}) in the device. On the other hand, Δn_T can be enhanced by increasing the thermal resistance of the silicon microring resonator.

II. ETCHLESS SILICON MICRORING RESONATOR

Equation (1) sets the guideline in designing the physical and geometrical properties of the resonator to relate the FCD blueshift and the TO redshift of the resonance. We can increase the FCD blueshift by designing a photonic structure with long free carrier lifetime (τ_{FC}) to compensate the dominant TO redshift. To achieve the long carrier lifetime, we avoid etching of the silicon waveguides by using an etchless process based on selective thermal oxidation of the silicon [6]. The etchless silicon waveguides are fabricated from a silicon-on-insulator (SOI) wafer with an initial silicon layer of 500 nm and a buried oxide layer (BOX) of 3 μm. First we grow a thermal oxide layer of 785 nm on the 500 nm SOI which consumes approximately 360 nm of silicon (see Fig. 1(a)). We then pattern 800 nm wide waveguides with electron beam (e-beam) lithography using ma-N 2405 resist. This pattern is transferred into the top oxide layer with reactive ion etching (RIE), where all but a thin slab of 50 nm of the oxide is removed (see Fig. 1(b)). This thin oxide slab is left behind so that the silicon is never exposed to the etching plasma, therefore preventing damage from the ion bombardment and chemical reactions that occur during plasma etching. After stripping the e-beam resist, we use thermal oxidation to define a 60 nm thick silicon waveguide and a 6 nm thick silicon slab (see Fig. 1(c)). Lastly, the waveguides are clad with 2 μm of plasma enhanced chemical vapor deposition (PECVD) oxide to confine the mode (see Fig. 1(d)). This etchless technique results in an ultra-smooth Si/SiO_2 interface and reduces absorption and recombination sites [7].

We measure the free carrier lifetime of the fabricated 50 μm radius etchless silicon microring resonator using a pump-probe optical experiment (see Fig. 2(a)). We couple into the microring an Er-fiber pulsed laser with 500 fs

pulses, a 25 MHz repetition rate, and a spectral width of 6 nm at its center wavelength, λ_{pump} = 1543 nm. The 52 W peak power pump pulse generates free carriers in the microring via TPA and results in a blueshift of the resonance. Concurrently, a quasi-TE polarized continuous laser (CW) weak probe laser is coupled in the microring. The exponential growth in Fig. 2(b) is linearly related to the recombination of the free carriers, and the experimental carrier lifetime is calculated to be 10 ns, which is more than 1 order of magnitude longer than that of a regular etched silicon microring [8].

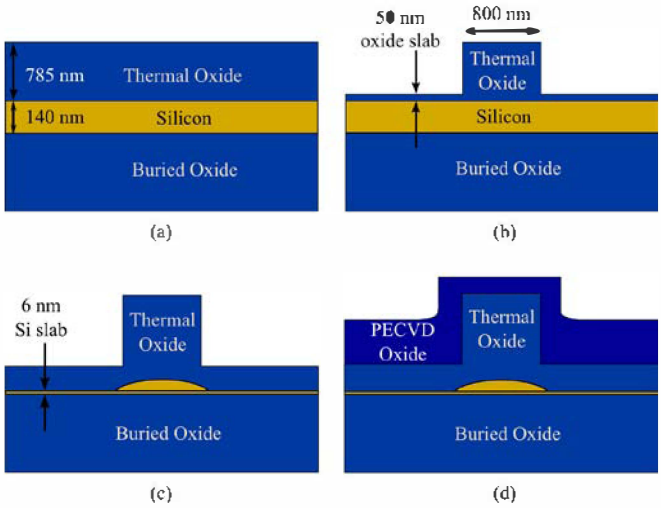

Fig. 1. Etchless fabrication process flow for low loss waveguides. (a) Growing of a thermal oxide layer of 785 nm, leaving behind 140 nm of silicon. (b) Patterning and etching of 800 nm wide waveguides, leaving behind a 50 nm oxide slab. (c) Thermal oxidation to define a 60 nm thick silicon waveguide with a 6 nm thick silicon slab. (d) Cladding of 2 μm thick PECVD oxide.

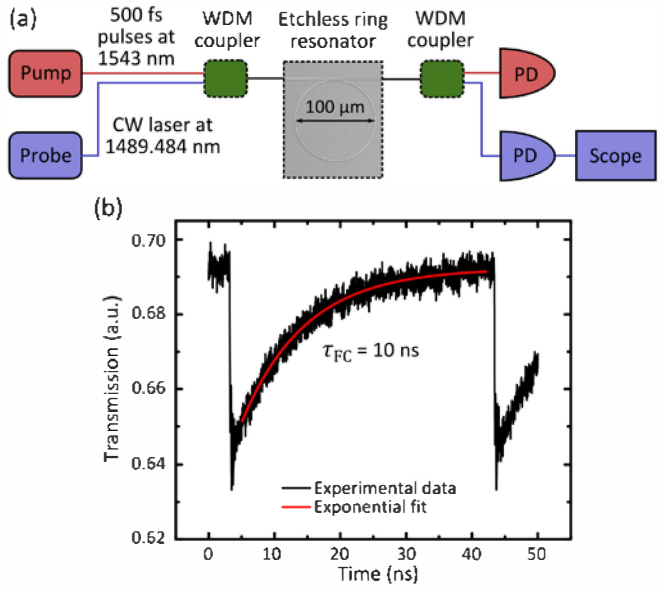

Fig. 2. (a) Schematic diagram of the pump-probe setup for the measurement of free carrier lifetime. (b) Experimental oscilloscope measurement of the carrier lifetime in etchless silicon microring resonator.

III. Engineering The Resonance Dependence

To tailor the resonance shift, we can engineer the thermal properties of the etchless silicon microring resonator as discussed in the previous section. In Fig. 3(a), we show the calculated resonant wavelength shift map of the etchless microring for a fixed τ_{FC} of 10 ns. We etch trenches around the microring to change the thermal resistance of the device (see Fig. 3(b)). By increasing the depth of the trenches (see Fig. 3(c)), the heat conductance of the microring decreases, thereby increases the thermal resistance. This leads to a stronger TO redshift.

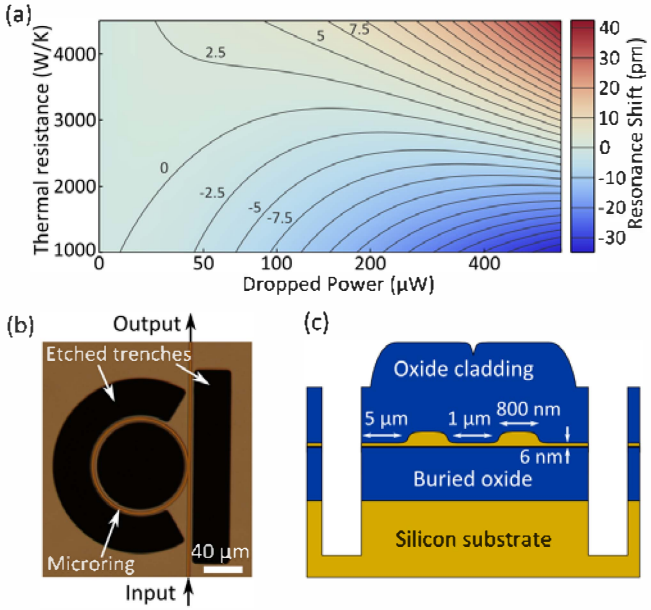

Fig. 3. (a) Density plot calculating the resonance shift as a function of thermal resistance and dropped power. (b) Optical microscope picture of the fabricated etchless silicon microring resonator with etched trenches. (c) Schematic diagram of the cross section to illustrate the depth of the trenches (not drawn to scale).

To analyze the effective resonance shift, we show in Fig. 4 the measured power-dependent resonant wavelength shift of three etchless silicon microrings; each device with a different depth of the etched trenches. Each curve in Fig. 4 is obtained by extracting the minimum transmission wavelength ($\lambda_0 \approx 1542$ nm) for different power levels of the scanning CW laser. In the resonator without trenches (R_{th} = 1300 K/W, blue curve in Fig. 4) there is a net blue shift, which becomes larger than one resonance linewidth at a dropped power around 30μW. By etching 300 μm deep trenches into the silicon substrate (R_{th} = 3800 K/W, see red curve in Fig. 4), there is a net red shift for dropped powers larger than 85 μW. This shows that the trenches significantly increase the thermal resistance of the device and the TO effect becomes the dominant process. By etching away only the 6 nm thin silicon slab (R_{th} = 3000 K/W, see green curve in Fig. 4), we obtain a power insensitive etchless silicon microring resonator for dropped power levels up to 335 μW. This represents a five-fold improvement in cavity energy handling capability, as compared to a regular etched microring [8].

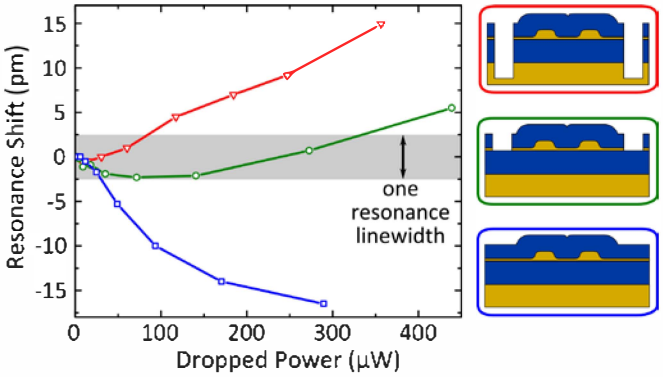

Fig. 4. Measured resonance shift power dependence (at $\lambda_0 \approx 1542$ nm) of three different etchless silicon microring resonator devices: one without etched trenches (blue curve), one with just the silicon slab etched (green curve), and one with 300μm deep trenches (red curve). The schematic insets on the right indicate the corresponding device cross-section.

IV. Conclusion

In conclusion, we tailor the microring resonator spectral dependence on input power by utilizing two counteracting processes, free carrier dispersion blue shift and thermo-optic red shift. In our fabricated devices, the resonant wavelength shifts less than one resonance linewidth for dropped power up to 335 μW, this represents a five-fold improvement in cavity energy handling capability, as compared to a regular etched microring. This compensation technique can also be employed in other resonator-based devices with long carrier lifetime [9].

Acknowledgment

This work was supported in part by the Defense Advanced Research Projects Agency (DARPA) under the Zeno-based OptoElectronics program, and award # W911NF-11-1-0435 supervised by Dr. Jagdeep Shah and the National Science Foundation under Grant No. 1143893 and was performed in part at the Cornell NanoScale Facility, a member of the National Nanotechnology Infrastructure Network, which is supported by the NSF. Lian-Wee Luo acknowledges a fellowship from Agency of Science, Technology and Research (A*STAR), Singapore.

References

[1] D. A. B. Miller, "Optical interconnects to silicon," *IEEE Journal of Selected Topics in Quantum Electronics,* vol. 6, pp. 1312-1317, Nov-Dec 2000.

[2] R. Soref, "The past, present, and future of silicon photonics," *IEEE Journal of Selected Topics in Quantum Electronics,* vol. 12, pp. 1678-1687, Nov-Dec 2006.

[3] M. Haurylau, *et al.*, "On-chip optical interconnect roadmap: Challenges and critical directions," *IEEE Journal of Selected Topics in Quantum Electronics,* vol. 12, pp. 1699-1705, Nov-Dec 2006.

[4] P. E. Barclay, K. Srinivasan, and O. Painter, "Nonlinear response of silicon photonic crystal microresonators excited via an integrated waveguide and fiber taper," *Optics Express,* vol. 13, pp. 801-820, Feb 7 2005.

[5] M. Soltani, "Novel Integrated Silicon Nanophotonic Structures using Ultra-high Q Resonators," Ph.D Thesis (Georgia Institute of Technology, 2009).

[6] J. Cardenas, *et al.*, "Low loss etchless silicon photonic waveguides," *Optics Express,* vol. 17, pp. 4752-4757, Mar 16 2009.

[7] L. W. Luo, G. S. Wiederhecker, J. Cardenas, C. Poitras, and M. Lipson, "High quality factor etchless silicon photonic ring resonators," *Optics Express,* vol. 19, pp. 6292-6297, Mar 28 2011.

[8] V. R. Almeida, C. A. Barrios, R. R. Panepucci, and M. Lipson, "All-optical control of light on a silicon chip," *Nature,* vol. 431, pp. 1081-1084, Oct 28 2004.

[9] J. van Campenhout, *et al.*, "Silicon-nitride surface passivation of submicrometer silicon waveguides for low-power optical switches," *Optics Letters,* vol. 34, pp. 1534-1536, May 15 2009.